Interaction between an Optically Levitated Nanoparticle and Its Thermal Image: Internal Thermometry via Displacement Sensing

Thomas Agrenius, Carlos Gonzalez-Ballestero, Patrick Maurer, and Oriol Romero-Isart
Institute for Quantum Optics and Quantum Information of the Austrian Academy of Sciences, A-6020 Innsbruck, Austria and Institute for Theoretical Physics, University of Innsbruck, A-6020 Innsbruck, Austria

(Received 3 October 2022; accepted 19 January 2023; published 28 February 2023)

We propose and theoretically analyze an experiment where displacement sensing of an optically levitated nanoparticle in front of a surface can be used to measure the induced dipole-dipole interaction between the nanoparticle and its thermal image. This is achieved by using a surface that is transparent to the trapping light but reflective to infrared radiation, with a reflectivity that can be time modulated. This dipole-dipole interaction relies on the thermal radiation emitted by a silica nanoparticle having sufficient temporal coherence to correlate the reflected radiation with the thermal fluctuations of the dipole. The resulting force is orders of magnitude stronger than the thermal gradient force, and it strongly depends on the internal temperature of the nanoparticle for a particle-to-surface distance greater than two micrometers. We argue that it is experimentally feasible to use displacement sensing of a levitated nanoparticle in front of a surface as an internal thermometer in ultrahigh vacuum. Experimental access to the internal physics of a levitated nanoparticle in vacuum is crucial to understanding the limitations that decoherence poses to current efforts devoted to preparing a nanoparticle in a macroscopic quantum superposition state.

DOI: 10.1103/PhysRevLett.130.093601

Today, it is experimentally possible to optically levitate a nanoparticle in vacuum [1] and (i) feedback cool its center-of-mass motion to the ground state [2–6], (ii) place it near a surface [7–13], (iii) measure the induced dipole-dipole interaction with another nanoparticle levitated in a second optical tweezer [14], and (iv) use displacement sensing to detect forces in the zeptonewton regime [15–21]. In this Letter, we propose to combine these experimental capabilities to measure the dipole-dipole interaction of an optically levitated nanoparticle with its *thermal* image [see Fig. 1(a)]. This interaction depends on the internal temperature of the nanoparticle for particle-to-surface distances comparable to the thermal wavelength. Hence, we propose to leverage displacement sensing for internal thermometry of a levitated nanoparticle in vacuum [22–26].

Our proposal aims not only at experimentally measuring an out-of-equilibrium Casimir force, which has been the object of intense research [30–37], but also at giving experimental access to the internal physics of a levitated nanoparticle in vacuum which is very relevant for the field of levitodynamics [1,38]. Knowledge of the internal temperature T of a nanoparticle and the imaginary part of its polarizability $\mathrm{Im}\{\alpha\}$ in the infrared regime is essential to quantify one of the most limiting sources of decoherence for experiments aiming to prepare a macroscopic quantum superposition of a nanoparticle [28,39–47]: decoherence due to thermal emission of photons [28,40,48,49]. The associated decoherence rate approximately scales with T^6 and critically depends on $\mathrm{Im}\{\alpha\}$. Furthermore, the assignment of an internal temperature to the nanoparticle in out-of-equilibrium situations assumes that the nanoparticle internally equilibrates faster than any other relevant timescale. This assumption (known as the local equilibrium assumption) underlies the current understanding of the internal physics of levitated nanoparticles and the associated sources of decoherence, but whether it holds for a nanoparticle in ultrahigh vacuum or not is a question that needs to be answered experimentally [50]. Our experimental proposal would test this assumption and its consequences.

More specifically, we propose to optically trap a silica glass nanoparticle of radius r and mass m at a distance z from a surface which is transparent at optical wavelengths but reflective at thermal (infrared) wavelengths, as illustrated in Fig. 1(a). We assume that the interaction between the nanoparticle and the electromagnetic field of wavelengths λ can be treated in the dipole approximation ($r \ll \lambda$) with isotropic polarizability $\alpha(\lambda)$, which we calculate from bulk electric permittivity data $\epsilon(\lambda)$ for silica glass [27] using $\alpha(\lambda) = 3V\epsilon_0[\epsilon(\lambda) - 1][\epsilon(\lambda) + 2]^{-1}$, where ϵ_0 is the vacuum permittivity and V the volume of the nanoparticle. We display $\mathrm{Im}\{\alpha(\lambda)\}$ for infrared and optical wavelengths in Fig. 1(c). To enable displacement sensing of the particle-surface interaction force, we propose to use a surface whose reflection coefficient can be modulated in time [51–55]. As illustrated in Fig. 1(b), we assume that the reflection coefficient [56] can be modulated around a high value in the infrared, while simultaneously being practically zero

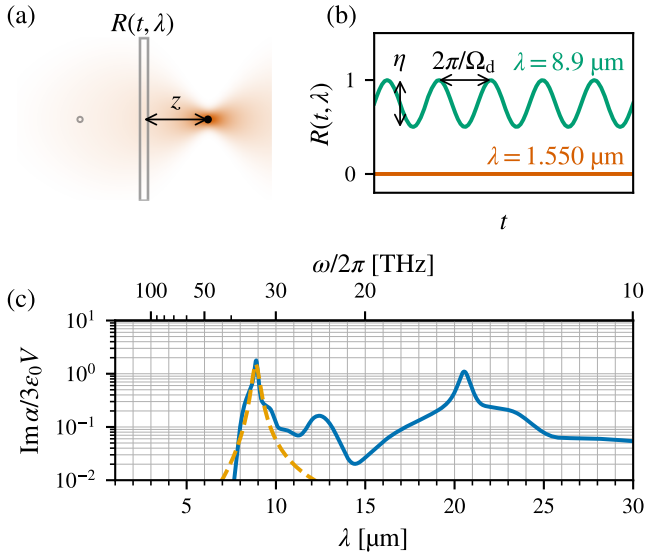

FIG. 1. (a) Illustration of the proposed experiment. A nanoparticle is optically trapped at a distance z from a surface with time- and wavelength-dependent reflection coefficient $R(t,\lambda)$. The effect of the surface can be approximated by the mirror image nanoparticle on the left. (b) The surface is transparent at the trapping wavelength, but the reflection coefficient can be modulated in time between high and low values at the peak wavelength of the nanoparticle's thermal emission. The modulation is sinusoidal with frequency Ω_d and amplitude η. (c) The imaginary part of the polarizability of an SiO_2 nanoparticle in the optical and infrared region of the spectrum using the model of $\epsilon(\lambda)$ from Ref. [27] (solid line). For $\lambda \in [1,7]$ μm, the imaginary part of the polarizability is smaller than the lower limit of the graph [27]. At $\lambda = 1.550$ μm we use $\mathrm{Im}\{\alpha\}/(3\epsilon_0 V) = 1.5 \times 10^{-9}$ based on data reported in Refs. [28,29]. The properties of the nanoparticle's infrared radiation is dominated by the peak at 8.9 μm, to which we fit a Lorentzian function (dashed line).

and without modulation at the optical wavelength. As we discuss quantitatively later, high and unmodulated transparency at the optical wavelength is necessary to avoid the influence of an interaction force between the nanoparticle and its optical image in the force sensing experiment [14,57,58]. Similarly, since the charge on optically levitated nanoparticles can be controlled [66], we propose to use electrically neutral particles to avoid interactions with the electrostatic mirror image [10]. We note that all-optical cold damping schemes for electrically uncharged silica nanoparticles have recently been demonstrated [5,67].

In order to evaluate the force acting on the particle in this scenario, we use the theory of fluctuational electrodynamics [31–35,37,68]. The steps we perform are summarized as follows (more details are given in the Supplemental Material [58]): we treat the nanoparticle as an electric dipole $\mathbf{d}$ which has a part induced by the electric field $\mathbf{d}_{\mathrm{ind}}$ and a thermally fluctuating part $\mathbf{d}_{\mathrm{th}}$. The total electric field $\mathbf{E}$ is composed of a fluctuating field from the radiation of the nanoparticle $\mathbf{E}_{\mathrm{ind}}$, a second fluctuating field from thermal radiation from the environment $\mathbf{E}_{\mathrm{th}}$, and a nonfluctuating field due to the presence of the optical tweezer $\mathbf{E}_{\mathrm{tw}}$. The force acting on the nanoparticle is the expectation value of the standard force on an electric dipole in an electric field: $\mathbf{F} = \sum_{j\in\{x,y,z\}} \langle d_j(t) \nabla E_j(\mathbf{r}_0, t)\rangle$, where $\mathbf{r}_0$ is the equilibrium position of the dipole. To evaluate this expression, we diagonalize the total dipole moment $\mathbf{d}(t)$ and field $\mathbf{E}(\mathbf{r}_0, t)$ in terms of the input quantities $\mathbf{d}_{\mathrm{th}}$ and $\mathbf{E}_{\mathrm{th}}$, whose correlations we assume to be given by the fluctuation-dissipation theorem, and $\mathbf{E}_{\mathrm{tw}}$. This is possible by transforming to the frequency domain where $\mathbf{d}_{\mathrm{ind}}(\omega) = \alpha(\omega)\mathbf{E}(\mathbf{r}_0,\omega)$ and $\mathbf{E}_{\mathrm{ind}}(\mathbf{r},\omega) = \mathbb{G}(\mathbf{r},\mathbf{r}_0,\omega)\mathbf{d}(\omega)$, with $\omega = 2\pi c/\lambda$, c the speed of light in vacuum, and $\alpha(\omega)$ defined in terms of $\alpha(\lambda = 2\pi c/\omega)$ [see top axis of Fig. 1(c)]. Here $\mathbb{G}(\mathbf{r},\mathbf{r}_0,\omega)$ is the electromagnetic Green's tensor. The presence of the surface modifies the Green's tensor, adding a scattering part $\mathbb{G}_1$ to the free-space Green's tensor $\mathbb{G}_0$ so that $\mathbb{G} = \mathbb{G}_0 + \mathbb{G}_1$. After diagonalization, one finds $\mathbf{d}(\omega) = \mathbb{T}(\mathbf{r}_0,\omega)\{\mathbf{d}_{\mathrm{th}}(\omega) + \alpha(\omega)[\mathbf{E}_{\mathrm{tw}}(\mathbf{r}_0,\omega) + \mathbf{E}_{\mathrm{th}}(\mathbf{r}_0,\omega)]\}$, and $\mathbf{E}(\mathbf{r},\omega) = \mathbf{E}_{\mathrm{tw}}(\mathbf{r},\omega) + \mathbf{E}_{\mathrm{th}}(\mathbf{r},\omega) + \mathbb{G}(\mathbf{r},\mathbf{r}_0,\omega)\mathbf{d}(\omega)$. The tensor $\mathbb{T}(\mathbf{r}_0,\omega) \equiv [\mathbb{1} - \alpha(\omega)\mathbb{G}_1(\mathbf{r}_0,\mathbf{r}_0,\omega)]^{-1}$ accounts for multiple reflections between the surface and the dipole. Since the subwavelength nanoparticle scatters radiation only weakly, reflections beyond the first order turn out to have a negligible impact on the forces, and one can approximate $\mathbb{T}(\mathbf{r}_0,\omega) \approx \mathbb{1}$. $\mathbf{F}$ can now be evaluated with the fluctuation-dissipation relations $\langle d_{j,\mathrm{th}}(\omega) d^*_{k,\mathrm{th}}(\omega')\rangle = 2\pi\hbar\delta(\omega-\omega')[2n(\omega,T)+1]\mathrm{Im}\{\alpha(\omega)\}\delta_{jk}$ and $\langle E_{j,\mathrm{th}}(\mathbf{r},\omega) E^*_{k,\mathrm{th}}(\mathbf{r}_0,\omega')\rangle = 2\pi\hbar\delta(\omega-\omega')[2n(\omega,T_{\mathrm{env}})+1]\mathrm{Im}\{G_{jk}(\mathbf{r},\mathbf{r}_0,\omega)\}$. Here $n(\omega,T)$ is the Bose–Einstein distribution, $\hbar$ is the reduced Planck's constant, and T and T_{env} are the temperatures of the nanoparticle and the electromagnetic environment, respectively. The quantities $\mathbf{E}_{\mathrm{th}}$, $\mathbf{d}_{\mathrm{th}}$, and $\mathbf{E}_{\mathrm{tw}}$ are assumed to have vanishing cross-correlations.

With this method, the total force $\mathbf{F}$ on the nanoparticle is found to have five contributions (see the Supplemental Material [58] for details): (1) the optical force from the optical tweezer; (2) an interaction force between the nanoparticle and its optical mirror image [57], which we neglect in accord with our assumption that the surface is sufficiently transparent at the optical wavelength [58]; (3) the zero-temperature Casimir force between the surface and the nanoparticle [69]; (4) a force due to interaction with environmental thermal radiation which depends on T_{env}, and (5) a force due to interaction between the nanoparticle and its reflected thermal radiation [31,35], or equivalently, its thermal mirror image. The last contribution depends on the nanoparticle internal temperature T, and we will denote it as

$$\mathbf{F}_{\mathrm{rad}}(T,z) = \frac{\mathbf{e}_z \hbar c}{4\pi\epsilon_0 z^4} \int_0^\infty \frac{d\lambda}{\lambda^2} \frac{\mathrm{Im}\{\alpha(\lambda)\} f(2\pi z/\lambda)}{\exp[2\pi\hbar c/(k_B T\lambda)] - 1}. \quad (1)$$

Here, $\mathbf{e}_z$ is the surface normal vector, k_B is Boltzmann's constant, and $f(x)$ is the oscillatory dimensionless function

$f(x) = \mathrm{Re}\{\exp(2ix)(-3+6ix+6x^2-4ix^3)\}$. The expressions of the other four contributions to $\mathbf{F}$ are given in the Supplemental Material [58].

In Fig. 2, we plot $\mathbf{e}_z \cdot \mathbf{F}$ as a function of z and T in the range 300 to 1500 K with increments of 100 K. We assume $T_{\mathrm{env}} = 300$ K. Note that therefore the black line ($T = 300$ K) corresponds to the equilibrium case. We find that as T is increased, the total force becomes dominated by the T-dependent fifth contribution $\mathbf{F}_{\mathrm{rad}}$. Only at the smallest distances $z \lesssim 2$ μm is the temperature dependence lost. This is due to the dominance of the zero-temperature Casimir force component over all the other force contributions at small separations [35,36,68]. At distances $z > 2$ μm, the force scales more slowly with distance than the z^{-5} scaling characteristic of zero-temperature Casimir–Polder forces [35,69]. Additionally, we observe that the force oscillates in sign along z with a temperature-independent period. The oscillations arise due to the peak at $\lambda_{\mathrm{peak}} = 8.9$ μm of $\mathrm{Im}\{\alpha(\lambda)\}$ (which is attributed to vibrations of the Si—O bond in silica glass [27]) dominating the integral in Eq. (1) for $T \gtrsim 400$ K. To confirm this explanation, we fit a Lorentzian function centered at λ_{peak} to $\mathrm{Im}\{\alpha(\lambda)\}$, finding that the fit has full width at half maximum (FWHM) of 0.4 μm [dashed curve in Fig. 1(c)]. In the inset of Fig. 2, we compare the total force calculated using the fitted and full $\mathrm{Im}\{\alpha(\lambda)\}$ [the two curves in Fig. 1(c)], finding excellent agreement when the temperature of the nanoparticle is above 400 K. We remark

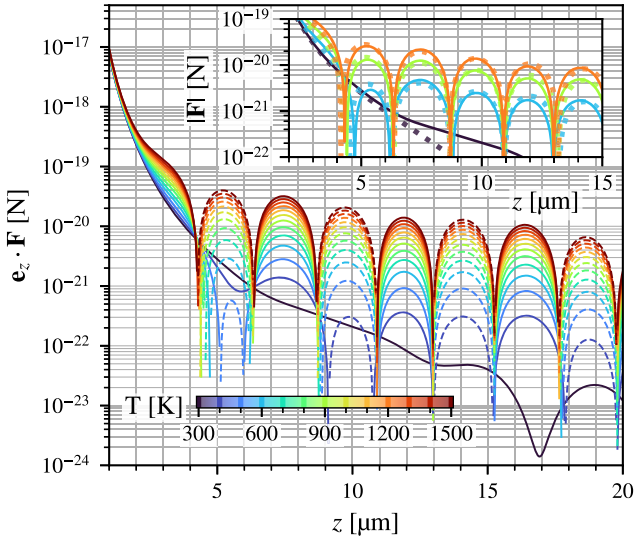

FIG. 2. The total dipole force on the nanoparticle along the direction normal to the surface when $R(t,\lambda) = 1$ for $\lambda \geq 7$ μm, using the full spectral dependence of $\alpha(\omega)$ [solid line in Fig. 1(c)]. Solid (dashed) lines indicate that the force is repulsive (attractive). The $T = 300$ K curve (black) is the force on the particle in equilibrium since we assume that $T_{\mathrm{env}} = 300$ K. Inset: Comparison of the total dipole force on the nanoparticle computed using the full spectral dependence (lines) versus the Lorentzian fit (dots) of $\alpha(\omega)$ as shown in Fig. 1(b).

that the oscillatory nature of the force could be utilized to perform a measurement of the distance from the nanoparticle to the surface.

We emphasize that the interaction giving rise to $\mathbf{F}_{\mathrm{rad}}$ is of a temporally coherent nature [14]. That is, the thermal dipole moment $\mathbf{d}_{\mathrm{th}}(t)$ remains correlated with itself during the time it takes for the thermally emitted radiation to be reflected by the surface and return to the particle: in the time domain, $\mathbf{E}_{\mathrm{ind}}(t) = \int_{-\infty}^{\infty} dt'\, \mathbb{G}(t-t')\,\mathbf{d}(t')$, and therefore $\mathbf{F}_{\mathrm{rad}} \propto \langle d_{\mathrm{th},j}(t) d_{\mathrm{th},k}(t')\rangle$. The temporal coherence of the nanoparticle's thermal radiation is endowed by the narrow frequency spectrum of $\mathrm{Im}\{\alpha\}$. A hypothetical increasingly broadband emitter, with accordingly shorter coherence time, would produce a force $\mathbf{F}_{\mathrm{rad}}$ with weakening oscillations which in the white-noise limit $\langle d_{\mathrm{th},j}(t) d_{\mathrm{th},k}(t')\rangle \to \delta(t-t')$ tends to zero since the time-domain Green's tensor vanishes for zero time argument. Additionally, we point out that $\mathbf{F}_{\mathrm{rad}}$ cannot be written as the gradient of an electromagnetic field intensity [70,71]. The gradient force that the nanoparticle experiences due to its radiated field intensity is a higher-order term in the tensor $\mathbb{T}(\mathbf{r}_0,\omega)$ which is not included in Eq. (1) and the contribution of which to $\mathbf{F}$ is negligible.

Figure 2 shows that $\mathbf{F}$ reaches values above 10^{-21} N, the currently demonstrated sensitivity in dynamic force sensing experiments with optically levitated nanoparticles in vacuum [2–4,15–17,19,21,72,73], for a wide range of temperatures T and particle-surface separations z. This suggests that $\mathbf{F}_{\mathrm{rad}}(T,z)$ can be measured with current laboratory capabilities. The thermally limited force sensitivity $\mathcal{S}$ is defined as $\mathcal{S} = \sqrt{S_{\mathrm{noise}}}$, where S_{noise} is the power spectral density (PSD) of the thermal forces acting on the nanoparticle. Under cold damping of the nanoparticle motion, the dominant sources of thermal noise are collisions with residual gas molecules and photon shot noise [73], and it can be shown that [58]

$$\mathcal{S} = \sqrt{\frac{2\hbar P_{\mathrm{scatt}}}{5c\lambda_0} + \frac{m\gamma_{\mathrm{gas}} k_B T_{\mathrm{env}}}{\pi}}. \tag{2}$$

Here P_{scatt} is the power that the nanoparticle scatters from the laser beam of wavelength λ_0 [73], and γ_{gas} is the damping rate due to collisions with gas molecules, directly proportional to the vacuum chamber pressure p [74]. We assume that the contributions from other sources of noise (e.g., surface-induced noise on neutral particles [75]) are negligible compared with the photon shot noise. In Fig. 3(a) we show that for the choice of experimental parameters presented in Table I, zeptonewton force sensitivity is achieved for $p \leq 10^{-9}$ mbar with saturation to the photon shot noise limit 4×10^{-22} N/$\sqrt{\mathrm{Hz}}$ at $p_{\mathrm{sat}} = 10^{-10}$ mbar. We assume this value of the pressure for the remainder of the discussion.

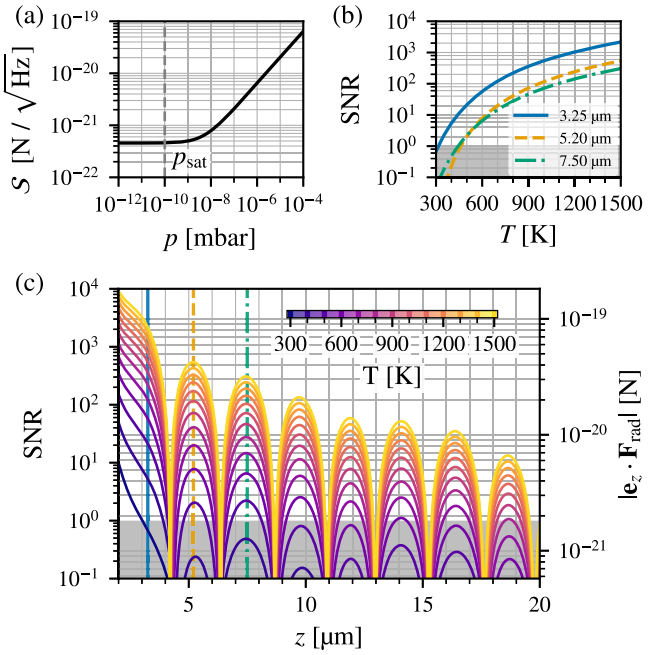

FIG. 3. (a) The force sensitivity as a function of the ambient gas pressure. The vertical dashed line identifies p_{sat}, the pressure below which the sensitivity is photon shot-noise limited. We use p_{sat} for plotting the other panels. (b) The signal-to-noise ratio (SNR) as a function of the nanoparticle internal temperature for three selected values of z. The gray area indicates the limit of measurability (SNR < 1). (c) The force (right y axis) and SNR (left y axis) as a function of z for $T = 300$ K, 400 K, …, 1500 K. The grid lines follow the force axis. The vertical lines indicate the selected values of z for which the full T dependence is displayed in panel (b).

In order to generate a time-oscillating T-dependent force that can be dynamically sensed [1], the reflection coefficient of the surface around the wavelength λ_{peak} is modulated as $R(t,\lambda) = 1 - \eta[1 - \cos(\Omega_d t)]/2$ [Fig. 1(b)]. By assuming that $\partial_\lambda R(t,\lambda) = 0$ across the 0.4 μm FWHM of the peak in $\text{Im}\{\alpha(\lambda)\}$ at λ_{peak}, $\mathbf{F}_{\text{rad}}$ splits into an average force and a time-dependent force $\eta|\mathbf{F}_{\text{rad}}(T,z)|\cos(\Omega_d t)/2$ [58]. The result is the appearance of a peak in the nanoparticle's motional PSD at the frequency Ω_d whose maximum is proportional to $|\mathbf{F}_{\text{rad}}(T,z)|^2$. The Ω_d frequency component of the reflection coefficient at the optical wavelength $R(t,\lambda_0)$, which we define as η_0, must simultaneously be kept small to avoid a similar and competing contribution to the motional PSD from the optical mirror image interaction force. More precisely, we require $\eta_0/\eta < |\mathbf{F}_{\text{rad}}|/|\mathbf{F}_{\text{cs}}|$, where $\mathbf{F}_{\text{cs}}$ is the force the nanoparticle would experience due to its interaction with its optical mirror image in a perfectly reflecting surface. As we show in the Supplemental Material [58], the ratio $|\mathbf{F}_{\text{rad}}|/|\mathbf{F}_{\text{cs}}| \sim 10^{-4}$, and we therefore require $\eta_0/\eta < 10^{-4}$. An experimentally feasible method to achieve this is to use metasurface optical filters [51,52,55,76–79]; see the Supplemental Material [58] for further details. When this requirement is fulfilled, the ratio of the Ω_d peak to the thermally driven motional PSD defines the signal-to-noise ratio (SNR), which for $p \leq p_{\text{sat}}$ becomes [58]

$$\text{SNR}(\Omega_d) = \frac{15c\epsilon_0^2}{256\pi^4\hbar}\frac{\lambda_0^7 Q\eta^2|\mathbf{F}_{\text{rad}}(T,z)|^2}{\Omega_d|\alpha(\lambda_0)|^2N^2P_{\text{tw}}}. \tag{3}$$

Here Q is the quality factor of the reflection coefficient modulation, and P_{tw} is the optical tweezer power. We plot the SNR as a function of T in Fig. 3(b) and as a function of z in Fig. 3(c). Figure 3(b) shows that the force is measurable (SNR > 1) in the entire temperature range 300–1500 K for $z = 3.25$ μm, and at least in the range 400–1500 K for $z = 7.50$ μm. In Fig. 3(c), we observe that with the chosen parameters, the force remains measurable for temperatures above 800 K even at separations of 19 μm and above. Additionally, we see in Fig. 3(b) that the SNR depends strongly on the internal temperature T, changing by several orders of magnitude (depending on z) as the temperature is increased by a factor of 5.

These results show that measurement of the driven $\mathbf{F}_{\text{rad}}$ provides a way to perform thermometry of the nanoparticle's internal temperature in ultrahigh vacuum [22–26]. Because of the absence of internal cooling by residual gas at p_{sat}, the main heat dissipation channel of the nanoparticle will be radiative cooling. This opens up the prospect of investigating the radiative thermalization of the nanoparticle, similar to what was done for a silica nanofiber in Ref. [80], but here for an isolated (i.e., unclamped) nanosized object. It was recently argued that the radiative thermalization of a highly isolated nanoparticle might differ from the predictions of fluctuational electrodynamics due to failure of the local equilibrium assumption during thermalization [50]. Qualitatively, the internal temperature of a subwavelength silica nanoparticle with polarizability as in Fig. 1(c) and which is being heated by laser absorption and cooled radiatively is predicted by fluctuational electrodynamics to obey [58]

TABLE I. Table of proposed experimental parameters.

Parameter	Value
Nanoparticle radius r	100 nm
Nanoparticle density ρ	2200 kg m^{-3}
Environment temperature T_{env}	300 K
Gas pressure p_{sat}	10^{-10} mbars
Tweezer wavelength λ_0	1.550 μm
Numerical aperture N	0.75
Laser power P_{tw}	10 mW
Reflection modulation amplitude η	0.5
Driving frequency Ω_d	$2\pi \times 12$ kHz
Driving quality factor Q	10^6

$$T(t)=\begin{cases} T_\infty \tanh\left[t/\tau+\operatorname{artanh}(T_0/T_\infty)\right] & (T_\infty > T_0) \\ T_\infty \coth\left[t/\tau+\operatorname{artanh}(T_\infty/T_0)\right] & (T_\infty < T_0) \end{cases}. \quad (4)$$

Here, T_0 and T_∞ are the temperatures at $t=0$ and $t=\infty$, respectively, and τ is a time constant which depends only on the properties of silica glass and the optical tweezer parameters but is independent of the subwavelength particle size. With the polarizability of Fig. 1(c) and parameters as in Table I, we find $T_\infty \approx 500$ K and $\tau \approx 0.2$ s. In experiments, T_0 can be independently controlled by using a dedicated heating laser [25]. By combining our proposed thermometry scheme with such a setup, departures from the radiative cooling described by Eq. (4), as predicted in Ref. [50], could be experimentally tested.

To conclude, we have proposed an experiment to measure an out-of-equilibrium Casimir force using an optically levitated nanoparticle in ultrahigh vacuum. We believe this is interesting *per se* given the challenge to measure these forces [36,37,81]. In addition, we have discussed how dynamic sensing of this force can be used to measure the internal temperature of the nanoparticle, both in the steady state as well as in a dynamical setting with radiative cooling taking place. This complements previous methods for measuring the internal temperatures of levitated nanoparticles, requiring either higher pressures [22,25] or nanoparticles with embedded quantum emitters [23,26,82]. Despite operating in the classical regime, we view the proposed experiment as highly relevant for current efforts to prepare large quantum superposition states of a levitated nanoparticle [28,39–47]. The design of these protocols is constrained by decoherence due to thermal radiation. One can show that this decoherence rate is proportional to $\int_0^\infty d\lambda\ \lambda^{-7} n(T,\lambda)\mathrm{Im}\{\alpha(\lambda)\}$ [49,83], and hence critically depends on both the nanoparticle's internal temperature and polarizability at infrared frequencies. Our proposed experiment gives information about both properties; the latter since the decoherence rate shows a similar dependence on $\alpha(\lambda)$ as Eq. (1). In addition, the observation that the thermal radiation of the nanoparticle is dominated by a narrow wavelength range would enable new strategies for the management of center-of-mass decoherence. We are currently investigating the effect on the decoherence rate of suppressing the radiation at the peak thermal wavelength. We hope this Letter will trigger the realization of classical experiments with levitated nanoparticles that provide key information about the physics related to sources of decoherence, which we consider pivotal in enabling the ambitious goal of preparing a nanoparticle in a large quantum superposition state.

We thank Romain Quidant for suggesting to us the idea of modulating the surface reflection coefficient. This research has been supported by the European Research Council (ERC) under Grant Agreement No. [951234] (Q-Xtreme ERC-2020-SyG).

[1] C. Gonzalez-Ballestero, M. Aspelmeyer, L. Novotny, R. Quidant, and O. Romero-Isart, Levitodynamics: Levitation and control of microscopic objects in vacuum, Science **374**, eabg3027 (2021).
[2] U. Delić, M. Reisenbauer, K. Dare, D. Grass, V. Vuletić, N. Kiesel, and M. Aspelmeyer, Cooling of a levitated nanoparticle to the motional quantum ground state, Science **367**, 892 (2020).
[3] L. Magrini, P. Rosenzweig, C. Bach, A. Deutschmann-Olek, S. G. Hofer, S. Hong, N. Kiesel, A. Kugi, and M. Aspelmeyer, Real-time optimal quantum control of mechanical motion at room temperature, Nature (London) **595**, 373 (2021).
[4] F. Tebbenjohanns, M. L. Mattana, M. Rossi, M. Frimmer, and L. Novotny, Quantum control of a nanoparticle optically levitated in cryogenic free space, Nature (London) **595**, 378 (2021).
[5] M. Kamba, R. Shimizu, and K. Aikawa, Optical cold damping of neutral nanoparticles near the ground state in an optical lattice, Opt. Express **30**, 26716 (2022).
[6] A. Ranfagni, K. Børkje, F. Marino, and F. Marin, Two-dimensional quantum motion of a levitated nanosphere, Phys. Rev. Res. **4**, 033051 (2022).
[7] I. Alda, J. Berthelot, R. A. Rica, and R. Quidant, Trapping and Manipulation of Individual Nanoparticles in a Planar Paul Trap, Appl. Phys. Lett. **109**, 163105 (2016).
[8] S. Kuhn, G. Wachter, F.-F. Wieser, J. Millen, M. Schneider, J. Schalko, U. Schmid, M. Trupke, and M. Arndt, Nanoparticle detection in an open-access silicon microcavity, Appl. Phys. Lett. **111**, 253107 (2017).
[9] R. Diehl, E. Hebestreit, R. Reimann, F. Tebbenjohanns, M. Frimmer, and L. Novotny, Optical levitation and feedback cooling of a nanoparticle at subwavelength distances from a membrane, Phys. Rev. A **98**, 013851 (2018).
[10] G. Winstone, R. Bennett, M. Rademacher, M. Rashid, S. Buhmann, and H. Ulbricht, Direct measurement of the electrostatic image force of a levitated charged nanoparticle close to a surface, Phys. Rev. A **98**, 053831 (2018).
[11] L. Magrini, R. A. Norte, R. Riedinger, I. Marinković, D. Grass, U. Delić, S. Gröblacher, S. Hong, and M. Aspelmeyer, Near-field coupling of a levitated nanoparticle to a photonic crystal cavity, Optica **5**, 1597 (2018).
[12] K. Shen, Y. Duan, P. Ju, Z. Xu, X. Chen, L. Zhang, J. Ahn, X. Ni, and T. Li, On-chip optical levitation with a metalens in vacuum, Optica **8**, 1359 (2021).
[13] C. Montoya, E. Alejandro, W. Eom, D. Grass, N. Clarisse, A. Witherspoon, and A. A. Geraci, Scanning force sensing at micrometer distances from a conductive surface with nanospheres in an optical lattice, Appl. Opt. **61**, 3486 (2022).
[14] J. Rieser, M. A. Ciampini, H. Rudolph, N. Kiesel, K. Hornberger, B. A. Stickler, M. Aspelmeyer, and U. Delić, Tunable light-induced dipole-dipole interaction between optically levitated nanoparticles, Science **377**, 987 (2022).

[15] T. Li, S. Kheifets, and M. G. Raizen, Millikelvin cooling of an optically trapped microsphere in vacuum, Nat. Phys. **7**, 527 (2011).
[16] J. Gieseler, B. Deutsch, R. Quidant, and L. Novotny, Subkelvin Parametric Feedback Cooling of a Laser-Trapped Nanoparticle, Phys. Rev. Lett. **109**, 103603 (2012).
[17] J. Gieseler, L. Novotny, and R. Quidant, Thermal nonlinearities in a nanomechanical oscillator, Nat. Phys. **9**, 806 (2013).
[18] D. C. Moore, A. D. Rider, and G. Gratta, Search for Millicharged Particles Using Optically Levitated Microspheres, Phys. Rev. Lett. **113**, 251801 (2014).
[19] G. Ranjit, M. Cunningham, K. Casey, and A. A. Geraci, Zeptonewton force sensing with nanospheres in an optical lattice, Phys. Rev. A **93**, 053801 (2016).
[20] A. D. Rider, D. C. Moore, C. P. Blakemore, M. Louis, M. Lu, and G. Gratta, Search for Screened Interactions Associated with Dark Energy Below the 100 μm Length Scale, Phys. Rev. Lett. **117**, 101101 (2016).
[21] D. Hempston, J. Vovrosh, M. Toroš, G. Winstone, M. Rashid, and H. Ulbricht, Force sensing with an optically levitated charged nanoparticle, Appl. Phys. Lett. **111**, 133111 (2017).
[22] J. Millen, T. Deesuwan, P. Barker, and J. Anders, Nanoscale temperature measurements using non-equilibrium Brownian dynamics of a levitated nanosphere, Nat. Nanotechnol. **9**, 425 (2014).
[23] T. M. Hoang, J. Ahn, J. Bang, and T. Li, Electron spin control of optically levitated nanodiamonds in vacuum, Nat. Commun. **7**, 12250 (2016).
[24] T. Delord, L. Nicolas, M. Bodini, and G. Hétet, Diamonds levitating in a Paul trap under vacuum: Measurements of laser-induced heating via NV center thermometry, Appl. Phys. Lett. **111**, 013101 (2017).
[25] E. Hebestreit, R. Reimann, M. Frimmer, and L. Novotny, Measuring the internal temperature of a levitated nanoparticle in high vacuum, Phys. Rev. A **97**, 043803 (2018).
[26] F. Rivière, T. de Guillebon, L. Maumet, G. Hétet, M. Schmidt, J.-S. Lauret, and L. Rondin, Thermometry of an optically levitated nanodiamond, AVS Quantum Sci. **4**, 030801 (2022).
[27] R. Kitamura, L. Pilon, and M. Jonasz, Optical constants of silica glass from extreme ultraviolet to far infrared at near room temperature, Appl. Opt. **46**, 8118 (2007).
[28] J. Bateman, S. Nimmrichter, K. Hornberger, and H. Ulbricht, Near-field interferometry of a free-falling nanoparticle from a point-like source, Nat. Commun. **5**, 4788 (2014).
[29] H. Lee, T. Chen, J. Li, O. Painter, and K. J. Vahala, Ultra-low-loss optical delay line on a silicon chip, Nat. Commun. **3**, 867 (2012).
[30] J. M. Obrecht, R. J. Wild, M. Antezza, L. P. Pitaevskii, S. Stringari, and E. A. Cornell, Measurement of the Temperature Dependence of the Casimir-Polder Force, Phys. Rev. Lett. **98**, 063201 (2007).
[31] C. Henkel, K. Joulain, J.-P. Mulet, and J.-J. Greffet, Radiation forces on small particles in thermal near fields, J. Opt. A **4**, S109 (2002).
[32] M. Antezza, L. P. Pitaevskii, and S. Stringari, New Asymptotic Behavior of the Surface-Atom Force Out of Thermal Equilibrium, Phys. Rev. Lett. **95**, 113202 (2005).
[33] M. Antezza, L. P. Pitaevskii, S. Stringari, and V. B. Svetovoy, Casimir-Lifshitz Force Out of Thermal Equilibrium and Asymptotic Nonadditivity, Phys. Rev. Lett. **97**, 223203 (2006).
[34] M. Antezza, L. P. Pitaevskii, S. Stringari, and V. B. Svetovoy, Casimir-Lifshitz force out of thermal equilibrium, Phys. Rev. A **77**, 022901 (2008).
[35] M. Krüger, T. Emig, G. Bimonte, and M. Kardar, Non-equilibrium Casimir forces: Spheres and sphere-plate, Europhys. Lett. **95**, 21002 (2011).
[36] G. Bimonte, Observing the Casimir-Lifshitz force out of thermal equilibrium, Phys. Rev. A **92**, 032116 (2015).
[37] G. Bimonte, T. Emig, M. Kardar, and M. Krüger, Non-equilibrium fluctuational quantum electrodynamics: Heat radiation, heat transfer, and force, Annu. Rev. Condens. Matter Phys. **8**, 119 (2017).
[38] C. Gonzalez-Ballestero, J. Gieseler, and O. Romero-Isart, Quantum Acoustomechanics with a Micromagnet, Phys. Rev. Lett. **124**, 093602 (2020).
[39] O. Romero-Isart, A. C. Pflanzer, F. Blaser, R. Kaltenbaek, N. Kiesel, M. Aspelmeyer, and J. I. Cirac, Large Quantum Superpositions and Interference of Massive Nanometer-Sized Objects, Phys. Rev. Lett. **107**, 020405 (2011).
[40] O. Romero-Isart, Quantum superposition of massive objects and collapse models, Phys. Rev. A **84**, 052121 (2011).
[41] Z.-q. Yin, T. Li, X. Zhang, and L. M. Duan, Large quantum superpositions of a levitated nanodiamond through spin-optomechanical coupling, Phys. Rev. A **88**, 033614 (2013).
[42] C. Wan, M. Scala, G. W. Morley, A. A. Rahman, H. Ulbricht, J. Bateman, P. F. Barker, S. Bose, and M. S. Kim, Free Nano-Object Ramsey Interferometry for Large Quantum Superpositions, Phys. Rev. Lett. **117**, 143003 (2016).
[43] O. Romero-Isart, Coherent inflation for large quantum superpositions of levitated microspheres, New J. Phys. **19**, 123029 (2017).
[44] H. Pino, J. Prat-Camps, K. Sinha, B. P. Venkatesh, and O. Romero-Isart, On-chip quantum interference of a superconducting microsphere, Quantum Sci. Technol. **3**, 025001 (2018).
[45] B. A. Stickler, B. Papendell, S. Kuhn, B. Schrinski, J. Millen, M. Arndt, and K. Hornberger, Probing macroscopic quantum superpositions with nanorotors, New J. Phys. **20**, 122001 (2018).
[46] T. Weiss, M. Roda-Llordes, E. Torrontegui, M. Aspelmeyer, and O. Romero-Isart, Large Quantum Delocalization of a Levitated Nanoparticle Using Optimal Control: Applications for Force Sensing and Entangling Via Weak Forces, Phys. Rev. Lett. **127**, 023601 (2021).
[47] L. Neumeier, M. A. Ciampini, O. Romero-Isart, M. Aspelmeyer, and N. Kiesel, Fast quantum interference of a nanoparticle via optical potential control, arXiv:2207.12539.
[48] L. Hackermüller, K. Hornberger, B. Brezger, A. Zeilinger, and M. Arndt, Decoherence of matter waves by thermal emission of radiation, Nature (London) **427**, 711 (2004).

[49] M. A. Schlosshauer, *Decoherence and the Quantum-to-Classical Transition*, The Frontiers Collection (Springer, Berlin; London, 2007).

[50] A. E. Rubio López, C. Gonzalez-Ballestero, and O. Romero-Isart, Internal quantum dynamics of a nanoparticle in a thermal electromagnetic field: A minimal model, Phys. Rev. B **98**, 155405 (2018).

[51] L. Kang, R. P. Jenkins, and D. H. Werner, Recent progress in active optical metasurfaces, Adv. Opt. Mater. **7**, 1801813 (2019).

[52] T. Huang, X. Zhao, S. Zeng, A. Crunteanu, P. P. Shum, and N. Yu, Planar nonlinear metasurface optics and their applications, Rep. Prog. Phys. **83**, 126101 (2020).

[53] Y. Yao, R. Shankar, M. A. Kats, Y. Song, J. Kong, M. Loncar, and F. Capasso, Electrically tunable metasurface perfect absorbers for ultrathin mid-infrared optical modulators, Nano Lett. **14**, 6526 (2014).

[54] B. Zeng, Z. Huang, A. Singh, Y. Yao, A. K. Azad, A. D. Mohite, A. J. Taylor, D. R. Smith, and H.-T. Chen, Hybrid graphene metasurfaces for high-speed mid-infrared light modulation and single-pixel imaging, Light Sci. Appl. **7**, 51 (2018).

[55] A. Komar, Z. Fang, J. Bohn, J. Sautter, M. Decker, A. Miroshnichenko, T. Pertsch, I. Brener, Y. S. Kivshar, I. Staude, and D. N. Neshev, Electrically tunable all-dielectric optical metasurfaces based on liquid crystals, Appl. Phys. Lett. **110**, 071109 (2017).

[56] We define the reflection coefficient $R(t,\lambda)$ as the magnitude of the Fresnel reflection coefficient at normal incidence.

[57] L. Dania, K. Heidegger, D. S. Bykov, G. Cerchiari, G. Araneda, and T. E. Northup, Position Measurement of a Levitated Nanoparticle via Interference with its Mirror Image, Phys. Rev. Lett. **129**, 013601 (2022).

[58] See Supplemental Material at http://link.aps.org/supplemental/10.1103/PhysRevLett.130.093601, which includes Refs. [59–65], for further details on the derivation and evaluation of the forces on the nanoparticle including a derivation of Eq. (1); the Lorentzian approximation of the polarizability; the sensing of the thermal image force, including derivations of Eqs. (2) and (3); the experimental feasibility of the surface reflection modulation required by the proposal; and the radiative thermalization of the nanoparticle, including a derivation of Eq. (4).

[59] L. Novotny and B. Hecht, *Principles of Nano-Optics* (Cambridge University Press, Cambridge, England, 2006).

[60] J. M. Wylie and J. E. Sipe, Quantum electrodynamics near an interface, Phys. Rev. A **30**, 1185 (1984).

[61] P. Virtanen *et al.*, SciPy 1.0: Fundamental algorithms for scientific computing in Python, Nat. Methods **17**, 261 (2020).

[62] R. Piessens, E. de Doncker-Kapenga, C. W. Überhuber, and D. K. Kahaner, *Quadpack: A Subroutine Package for Automatic Integration* (Springer Science & Business Media, New York, 2012).

[63] M. M. Jadidi, J. C. König-Otto, S. Winnerl, A. B. Sushkov, H. D. Drew, T. E. Murphy, and M. Mittendorff, Nonlinear terahertz absorption of graphene plasmons, Nano Lett. **16**, 2734 (2016).

[64] C. Gonzalez-Ballestero, P. Maurer, D. Windey, L. Novotny, R. Reimann, and O. Romero-Isart, Theory for cavity cooling of levitated nanoparticles via coherent scattering: Master equation approach, Phys. Rev. A **100**, 013805 (2019).

[65] R. Messina, M. Tschikin, S.-A. Biehs, and P. Ben-Abdallah, Fluctuation-electrodynamic theory and dynamics of heat transfer in systems of multiple dipoles, Phys. Rev. B **88**, 104307 (2013).

[66] M. Frimmer, K. Luszcz, S. Ferreiro, V. Jain, E. Hebestreit, and L. Novotny, Controlling the net charge on a nanoparticle optically levitated in vacuum, Phys. Rev. A **95**, 061801(R) (2017).

[67] J. Vijayan, Z. Zhang, J. Piotrowski, D. Windey, F. van der Laan, M. Frimmer, and L. Novotny, Scalable all-optical cold damping of levitated nanoparticles, Nat. Nanotechnol. **18**, 49 (2023).

[68] S. Y. Buhmann, *Dispersion Forces. 1: Macroscopic Quantum Electrodynamics and Ground-State Casimir, Casimir-Polder and van Der Waals Forces*, Springer Tracts in Modern Physics No. 247 (Springer, Berlin Heidelberg, 2012).

[69] H. B. G. Casimir and D. Polder, The influence of retardation on the London-van der Waals forces, Phys. Rev. **73**, 360 (1948).

[70] M. Sonnleitner, M. Ritsch-Marte, and H. Ritsch, Attractive Optical Forces from Blackbody Radiation, Phys. Rev. Lett. **111**, 023601 (2013).

[71] P. Haslinger, M. Jaffe, V. Xu, O. Schwartz, M. Sonnleitner, M. Ritsch-Marte, H. Ritsch, and H. Müller, Attractive force on atoms due to blackbody radiation, Nat. Phys. **14**, 257 (2018).

[72] A. A. Geraci, S. B. Papp, and J. Kitching, Short-Range Force Detection Using Optically-Cooled Levitated Microspheres, Phys. Rev. Lett. **105**, 101101 (2010).

[73] V. Jain, J. Gieseler, C. Moritz, C. Dellago, R. Quidant, and L. Novotny, Direct Measurement of Photon Recoil from a Levitated Nanoparticle, Phys. Rev. Lett. **116**, 243601 (2016).

[74] S. A. Beresnev, V. G. Chernyak, and G. A. Fomyagin, Motion of a spherical particle in a rarefied gas. Part 2. Drag and thermal polarization, J. Fluid Mech. **219**, 405 (1990).

[75] M. E. Gehm, K. M. O'Hara, T. A. Savard, and J. E. Thomas, Dynamics of noise-induced heating in atom traps, Phys. Rev. A **58**, 3914 (1998).

[76] X. Wang, H. Meng, S. Liu, S. Deng, T. Jiao, Z. Wei, F. Wang, C. Tan, and X. Huang, Tunable graphene-based mid-infrared plasmonic multispectral and narrow band-stop filter, Mater. Res. Express **5**, 045804 (2018).

[77] Y. Wang, H. Liu, S. Wang, and M. Cai, Wide-range tunable narrow band-stop filter based on bilayer graphene in the mid-infrared region, IEEE Photonics J. **12**, 1 (2020).

[78] L. Ju, B. Geng, J. Horng, C. Girit, M. Martin, Z. Hao, H. A. Bechtel, X. Liang, A. Zettl, Y. R. Shen, and F. Wang, Graphene plasmonics for tunable terahertz metamaterials, Nat. Nanotechnol. **6**, 630 (2011).

[79] X. Shi, C. Chen, S. Liu, and G. Li, Nonvolatile, reconfigurable and narrowband mid-infrared filter based on surface lattice resonance in phase-change $Ge_2Sb_2Te_5$, Nanomater. Nanotechnol. **10**, 2530 (2020).

[80] C. Wuttke and A. Rauschenbeutel, Thermalization via Heat Radiation of an Individual Object Thinner Than the Thermal Wavelength, Phys. Rev. Lett. **111**, 024301 (2013).

[81] A. O. Sushkov, W. J. Kim, D. a. R. Dalvit, and S. K. Lamoreaux, Observation of the thermal Casimir force, Nat. Phys. **7**, 230 (2011).

[82] A. T. M. A. Rahman, A. C. Frangeskou, M. S. Kim, S. Bose, G. W. Morley, and P. F. Barker, Burning and graphitization of optically levitated nanodiamonds in vacuum, Sci. Rep. **6**, 21633 (2016).

[83] K. Hornberger, J. E. Sipe, and M. Arndt, Theory of decoherence in a matter wave Talbot-Lau interferometer, Phys. Rev. A **70**, 053608 (2004).